DOI: 10.16078/j.tribology.2022203

基于机器学习的金属材料划痕响应预测

秦瑾鸿[1], 张建伟[2*], 李元鑫[2], 曹向阳[1], 乔泽沅[1]
(1. 郑州大学 机械与动力工程学院, 河南 郑州 450001;
2. 郑州大学 力学与安全工程学院, 河南 郑州 450001)

摘 要: 确定材料的划痕响应对评价其抗划擦及摩擦磨损性能有着重要的价值. 采用有限元仿真与经典多输出多层感知器(MLP)神经网络的方法, 建立了划痕输入参量(材料的屈服应力、应变硬化指数和界面摩擦系数以及划痕过程中施加的法向加载力)与划痕响应(表观深度、划痕宽度以及划痕切向力)之间的关系. 由有限元结果与机器学习预测结果的对比可知: 采用960组金属材料划痕仿真数据集训练的MLP神经网络预测结果与有限元仿真结果吻合较好. 采用304不锈钢、黄铜和18CrNiMo7-6合金钢的划痕试验对MLP神经网络进行了试验验证. 结果表明: MLP神经网络预测的划痕响应与试验中获得的结果较为接近. 本文中结果可为评价材料抗划擦性能提供了1种可行的方法.

关键词: 机器学习; 划痕; 金属; 有限元分析; 力学性能
中图分类号: TB93 **文献标志码:** A **文章编号:** 1004-0595(2023)12–1445–08

Prediction of Scratch Responses of Metallic Material Based on Machine Learning

QIN Jinhong[1], ZHANG Jianwei[2*], LI Yuanxin[2], CAO Xiangyang[1], QIAO Zeyuan[1]

(*1. School of Mechanical and Power Engineering, Zhengzhou University, Henan Zhengzhou 450001, China;*
2. School of Mechanical and Safety Engineering, Zhengzhou University, Henan Zhengzhou 450001, China)

Abstract: Determining the scratch responses of metallic material plays a vital role in evaluating its resistance to scratching, friction and wearing. In the present study, finite element simulation was performed and the classical multi-layer perceptron (MLP) neural network method was used to explore the relationship between the input parameters in a scratch test (yield stress σ_y, strain hardening index n, interfacial friction coefficient μ_a, as well as the normal loading force F_n) and the scratch responses (apparent scratch depth d, scratch width w, and scratch tangential force F_t). The MLP neural network involved three parts: an input layer, hidden layers, and an output layer. Each layer in this model consists of many neurons, the neuronal behavior of which was described using the MP model (McCulloch-Pitts Model). Considering the time-consuming and costly process to obtain the dataset required for neural network training through experimental approach, finite element simulation was performed to obtain the scratch test dataset in this study. The plastic parameters of most metallic materials were covered by the selected range of values for yield stress and strain hardening index in the finite element simulation. A total of 960 scratch simulation cases are performed. The simulation dataset was randomly divided into three parts. Specifically, 60% of the data was included in the training set to learn the training neural network, 20% of the data, i.e, the validation set, was used to determine the optimal hyperparameters, and the remaining 20% in the dataset, i.e, the test set, was used to determine the generalization of the model. Herein, ReLU was chosen as the activation function because the linear correction unit (ReLU) activation function can speed up the

Received 30 September 2022, revised 3 March 2023, accepted 6 March 2023, available online 7 March 2023.
*Corresponding author. E-mail: zhangjianwei@zzu.edu.cn, Tel: +86-15225089080.
This project was supported by the National Natural Science Foundation of China (12072324) and the Excellent Youth Foundation of Henan Scientific Committee(212300410087).
国家自然科学基金项目(12072324)和河南省优秀青年科学基金项目(212300410087)资助.

training of the neural network model and effectively resolve gradient disappearance. The hyperbolic cosine loss function (Log-Cosh) was taken as the loss function. A search for 50,000 hyperparameter combinations was conducted on the open source platform pytorch using Optuna, and the models were assessed on the validation set, with the minimum Mean Absolute Percentage Error (MAPE) value as the optimal model hyperparameter. The best MLP fit for F_t, w and d predictions was 0.947, 0.986 and 0.97, respectively. Moreover, the MAPE of F_t falls below 11%, and that of w and d was smaller than 5.3% on both the training, validation, and test datasets, indicating the excellent predictability of the MLP. Scratch tests and tensile tests were conducted on 304 stainless steel, brass, and 18CrNiMo7-6 alloy steel to validate the trained MLP neural network. The results showed that the anti-scratch performance of the three materials used in the study range was ranked in the following order: 304 stainless steel > 18CrNiMo7-6 alloy steel > brass. This was because brass was less resistant to tensile deformation than 18CrNiMo7-6 alloy steel and 304 stainless steel. Although the yield stress of 304 stainless steel was lower than that of 18CrNiMo7-6 alloy steel, 304 stainless steel gradually outperforms 18CrNiMo7-6 alloy steel in the resistance to deformation with the increase in severity of tensile deformation. The relative errors of w and F_t of predicted scratch responsed from trained MLP neural network and scratch tests were within 10%, and the relative error of d was within 5%. The trained MLP neural network as proposed in this paper was applicable to make reasonable prediction of scratch responses for different metallic materials. Also, the results of this paper provided a viable solution to evaluating the anti-scratch performance of metallic materials.

Key words: machine learning; scratch; metal; finite element analysis; mechanical property

划痕法最初用来测试材料的硬度[1]，如今这种方法被广泛用于测量膜基结合力[2-4]、测定材料的断裂韧性[5-8]和塑性参数[9-10]以及研究材料的摩擦与磨损行为[11-13]. 为了指导设计具有良好抗划擦性能的材料，学者们开展了大量工作寻找材料的力学性能与其划痕行为之间关系[14-16]. 基于有限元仿真，Jiang等[17]发现屈服应力和界面摩擦系数是影响聚合物划痕响应的重要参数. Zhang等[18]采用划痕试验和有限元仿真相结合的方法，得出屈服强度大、弹性模量小的聚丙烯具有较好的抗划擦性能. Pöhl等[19]发现金属材料的应变硬化指数在划痕堆积形成中具有重要作用. Liu等[20]对比了划痕速度对不同恒定法向载荷下4种热塑性塑料划痕响应的影响. 由于划痕过程的复杂性，很难建立材料力学性能与划痕响应之间的定量关系.

神经网络(NNs)对于各个变量之间复杂的、不确定的以及非线性关系的强大处理能力[21]，为研究金属材料划痕响应提供了1种有效方法. NNs在许多领域取得了成功[22]，如视频图像分析[23]和自然语言处理[24]等. 此外，Liu等[25]用NNs来预测五边形截面悬臂梁的小尺度断裂韧性并且与回归树的方法进行了对比，结果表明NNs可以更简单地得到更准确的预测结果. Lu等[26]将NNs应用到压痕方法中，通过压痕结果逆分析得到1个可以预测材料力学性能的多保真度神经网络模型. Xie等[27]基于有限元仿真结果构造了NNs，分析出Ti-6Al-4V微纳米划痕过程中划痕深度与剪切摩擦系数无关，剪切摩擦系数与耕犁摩擦系数呈正相关.

本文中关注的问题是通过材料力学性能、加载工况确定材料的划痕响应，为多输入多输出的回归问题. 由于经典多输出多层感知器(MLP)神经网络具备高度的并行处理、高度的非线性全局作用和良好的容错性等优点，且具有良好的处理多输入多输出回归问题的能力，因此本文中基于有限元数据训练MLP神经网络来预测金属材料划痕响应. 选取切向力、表观深度[28](划痕堆积峰值到槽底的高度)、划痕宽度来评价抗划擦性能[17]. 训练的神经网络将建立起不同材料力学性能(屈服应力和应变硬化指数)、划痕工况(界面摩擦系数和法向力)与划痕响应(切向力、表观深度和划痕宽度)之间的关系. 本文作者为评价材料抗划擦性能提供1种可行的方法，同时展示神经网络在划痕研究中的应用潜能.

1 理论和有限元仿真

如图1所示，划痕测试过程为首先将压头压入试样，当达到设定的法向力F_n后，压头在恒定的法向力下以设定的划痕速度沿切向滑动. 在划痕过程中法向加载为恒定载荷，可用于表征材料的划痕硬度[29]和塑性性能[9, 30]. 除此之外，划痕试验还有渐进载荷的加载方式，主要应用于研究划痕失效[31]和确定断裂韧性[5, 8]. 切向运动起始阶段会出现1个瞬态的划痕响应，即摩擦系数等划痕响应出现较大的波动. 之后材料的划痕宽度、表观深度等趋于稳定，这时划痕测试达到稳定状态. 划痕稳定状态通常需要划痕距离达到划痕宽度的2~3倍[32]. 划痕测试采用维氏压头. 除了施加的法向力和划痕速度等参数，压头与材料之间的界面摩擦系数μ_a也会影响划痕结果. 在划痕测试结束后，可以得

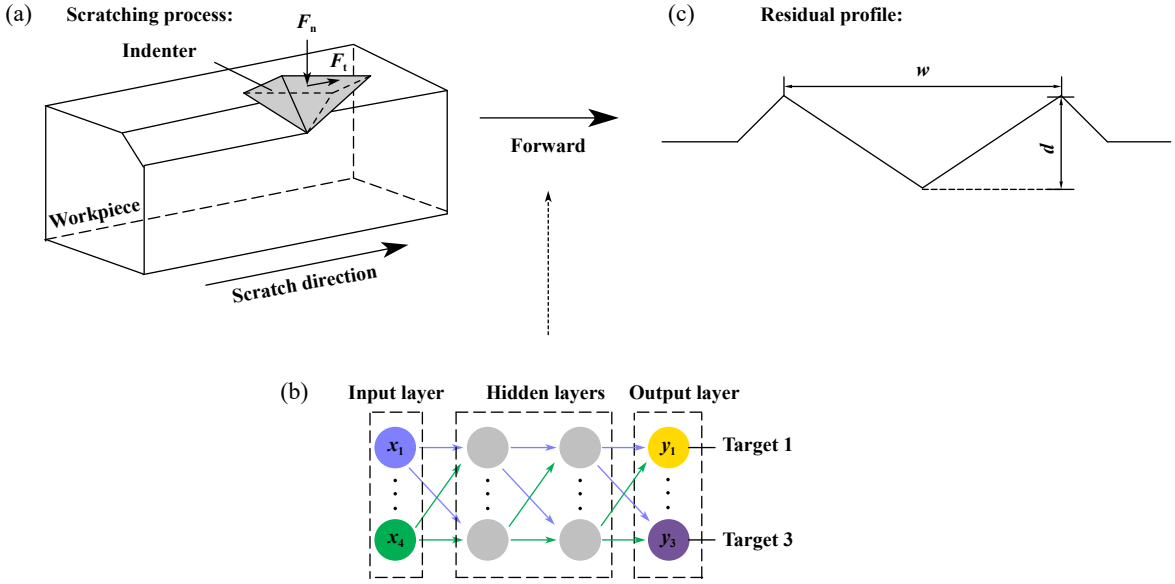

Fig. 1　A classic multi-output multi-layer perceptron(MLP): (a) schematic diagram of scratch test; (b) the structure of MLP for scratch simulations; (c) schematic diagram of residual profile

图 1　经典的多输出多层感知器神经网络示意图: (a)划痕试验示意; (b) MLP神经网络框架; (c)划痕残余形貌

到材料的划痕响应如: 残余划痕宽度w, 表观深度d以及切向力F_t, 如图1(a)和(c)所示. 大多数金属材料的塑性行为可由幂律函数来描述[32], 因此采用公式(1)来表示材料的应力应变关系[33]:

$$\begin{cases}\sigma = E\varepsilon & \varepsilon \leqslant \varepsilon_y \\ \sigma = E\varepsilon_y^{1-n}\varepsilon^n & \varepsilon > \varepsilon_y\end{cases} \tag{1}$$

其中, ε_y为屈服应变, E为弹性模量, σ_y为屈服应力, ε表示总应变包括塑性应变和弹性应变, n表示应变硬化指数.

MLP神经网络如图1(b)所示, 分为三部分: 输入层、隐藏层和输出层. 这个模型中每层由许多神经元组成, 采用MP模型(McCulloch-Pitts Model)来描述神经元行为. 神经元从上一层的所有神经元接收带权重的信号, 并将收到的总输入与阈值进行比较, 然后通过激活函数输入下一层的所有神经元, 但输入到输出层的神经元是没有激活函数的. 给定MLP神经网络训练需要的数据集, 权重$\omega_i (i = 1,2,\cdots,n)$和阈值$\theta$可以通过学习寻找到近似最优值. 基于训练后的MLP神经网络[图1(b)], 输入已知材料的塑性参数(σ_y, n)和划痕工况(F_n, μ_a), 可以预测出划痕响应(w, d , F_t).

在工程应用中, 获取大量的数据是深度学习的难点之一. 考虑到用试验的方法获得神经网络训练所需的数据集非常耗时且成本巨大, 因此本文中采用有限元仿真的方法获取划痕测试数据集. 使用显示动力学软件LS-DYNA进行划痕过程的数值仿真. 如图2所示, 采用面对称模型进行划痕仿真计算. 采用维氏压头, 设置为离散刚体. 仿真模型共有109 555个六面体网格单元. 同时考虑计算精度和计算效率的情况下, 只在划痕路径附近加密网格. 材料杨氏模量E=210 GPa, 泊松比ν=0.3. 使用如下机器学习方案[公式(2)]来解决本文中的问题:

$$\begin{cases}\text{Input variables}: \underline{x} = (x_1,x_2,x_3,x_4) = (\sigma_y, n, F_n, \mu_a) \\ \text{Target variables}: y = (y_1,y_2,y_3) = (w,d,F_t)\end{cases} \tag{2}$$

选取表1所列的取值范围, 其中屈服应力和应变硬化指数取值范围覆盖了大多数金属材料的塑性参数. 压头与试验试样之间的界面摩擦系数考虑不同材料的界面黏附情况. 在划痕仿真中划针划入材料后尖端与材料初始表面的距离(即划入深度)与法向力一一对应, 考虑到计算稳定性, 本文中有限元仿真部分采

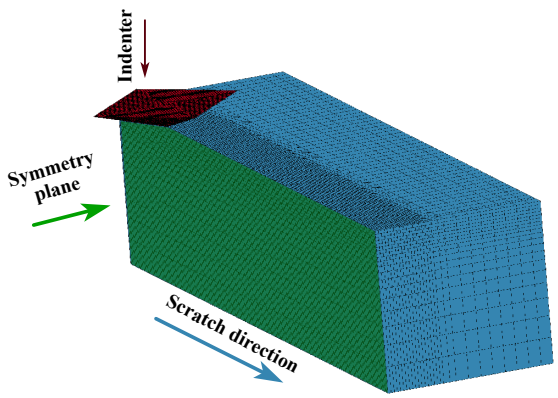

Fig. 2　Finite element model of scratch test

图 2　划痕试验的有限元模型

表 1 有限元仿真中的输入参数

Table 1 Input parameters in the finite element simulation

Input parameter	Range	Specifications
Yield stress, σ_y/MPa	100~2 000	100, 400, 600, 800, 1 100, 1 400, 1 700, 2 000
Strain hardening index, n	0.01~0.50	0.01, 0.1, 0.2, 0.3, 0.4, 0.5
Interfacial friction coefficient, μ_a	0.01~0.30	0.01, 0.1, 0.15, 0.2, 0.3
Scratch depth, h_d/μm	20~50	20, 30, 40, 50

用划入深度作为变量来代替法向力. 划痕长度为5 mm. 共有960组划痕仿真算例. 如图3所示，有限元切向运动起始阶段出现不稳定的划痕响应，所以有限元结果的取值为划痕响应稳定后5处取平均值.

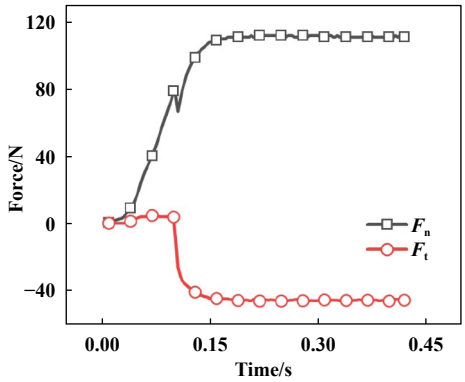

Fig. 3 Scratch normal and tangential forces at material parameters of yield stress 1 700 MPa, strain hardening index 0.4, interfacial coefficient of friction 0.2, and scratch depth 20 μm

图 3 材料参数为屈服应力1 700 MPa，应变硬化指数0.4，界面摩擦系数0.2，划入深度20 μm时的划痕法向力和切向力

2 试验材料与方法

对18CrNiMo7-6合金钢、304不锈钢和黄铜进行单轴拉伸和划痕试验以及界面摩擦系数测量. 单轴拉伸试验采用MTS Landmark 370.25，位移加载速率为0.45 mm/min. 3种材料试样尺寸如下：18CrNiMo7-6合金钢标距25 mm，直径6 mm，黄铜试样标距为50 mm，截面尺寸10 mm×2 mm，304不锈钢试样标距100 mm，直径10 mm. 划痕试验使用带有维氏压头的NANOVEA PB1000微纳米力学测试系统. 3种金属施加的划痕法向载荷均为24 N，划痕速度以1 mm/min加载，长度为5 mm，且保证相邻2条划痕之间的距离大于3倍划痕宽度. 每个测试条件下，重复进行3次拉伸和划痕试验. 用NPFLEX三维表面形貌仪测量表观深度和划痕宽度. 界面摩擦测试同样在NANOVEA PB1000微纳米力学测试系统进行. 使用金刚石平压头在平坦的试样表面上进行界面摩擦系数μ_a的测量，施加在平压头的法向载荷为0.5 N，滑动距离设置为10 mm.

3 结果与讨论

3.1 材料拉伸性能和界面摩擦系数

图4所示为18CrNiMo7-6合金钢、304不锈钢和黄铜拉伸试验得到的真应力应变曲线. 可以得出18CrNiMo7-6合金钢弹性模量为196±0.76 GPa，屈服应力385±10 MPa，应变硬化指数0.19±0.012；304不锈钢弹性模量为195±0.60 GPa，屈服应力和应变硬化指数分别为302±1 MPa和0.32±0.012；黄铜弹性模量为89±0.34 GPa，屈服应力和应变硬化指数分别为240±4 MPa和0.22±0.008. 金刚石和18CrNiMo7-6合金钢、304不锈钢以及黄铜的界面摩擦系数分别为0.12±0.015、0.11±0.009和0.16±0.011. 可见金刚石-304不锈钢摩擦副界面摩擦系数最小，金刚石-黄铜摩擦副界面摩擦系数最大.

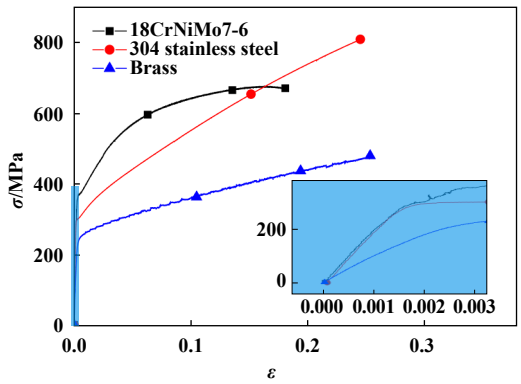

Fig. 4 Stress-strain results of 18CrNiMo7-6 alloy steel, 304 stainless steel and brass

图 4 18CrNiMo7-6合金钢、304不锈钢和黄铜的应力-应变曲线

3.2 MLP神经网络训练与预测

仿真数据集被随机分成了3个部分. 其中60%的数据用于训练集来学习训练神经网络，20%的数据用于验证集来判断最优的超参数，剩余的20%数据用于测试集，来判断模型的泛化性，其中测试集和验证集的数据神经网络并未进行学习. 考虑到线性修正单元(ReLU)激活函数可以加快NNs训练速度和有效解决梯度消失

问题，本文中选择ReLU作为激活函数. 选取双曲余弦损失函数(Log-Cosh)作为损失函数，选取平均绝对百分比误差(MAPE)直观评估模型的优劣，如公式(3)所示：

$$\mathrm{MAPE}=\frac{1}{N}\sum_{i=1}^{N}\left|\frac{\hat{y}(x)_i-y_i}{y_i}\right| \tag{3}$$

其中，$\hat{y}(x)_i$是预测值，y_i是实际i^{th}目标值，N表示数据集的数量.

超参数是指在训练机器学习模型之前必须设定的参数，常见的超参数包括隐藏层层数、隐藏层单元个数、学习率以及优化算法等. 这些参数通常用于控制模型的复杂度，以及模型在训练过程中的行为. 在设计神经网络时，通常会设定多个隐藏层，并且每层的单元数可以不同. 一般来说，隐藏层的单元数越多，模型的表示能力就越强，但同时也会增加训练的复杂度和运算量. 因此，在设计神经网络时，需要权衡模型的表示能力和训练复杂度，合理设定隐藏层的单元数. 学习率控制着模型在训练过程中权值和偏差的更新幅度. “Adam”、“RMSprop”和“SGD”是3种常见的优化算法. Adam是通过梯度和动量来调整学习率，RMSprop通过梯度的平方值来调整学习率，SGD只通过梯度来调整学习率. 为了寻找到近似最优的超参数：隐藏层数，每层单元的个数，学习步长和适合的自适应优化算法，采用Optuna[34]在开源平台Pytorch[35]上进行自动超参数寻找. 超参数搜索范围选取列于表2中，包含了神经网络隐藏层层数搜索范围、每层隐藏层神经元个数搜索范围、学习率搜索范围和3种优化算法. 根据数据集的大小选择基于核函数拟合的贝叶斯优化算法寻找最优的超参数组合.

表 2　MLP超参数的选取范围

Table 2　Range of hyperparameters for MLP

Model	MLP
Number of hidden layer	[1, 15]
Number of units per layer	[4, 128]
Learning rate	[1e-6, 1e-2]
Optimizer	Adam, RMSprop, SGD

MLP神经网络经过5万种超参数组合的搜索，并在验证集上对模型进行优劣判断，最小MAPE值为最优模型超参数. 最终给出了模型的最佳超参数组合，如图5所示，该模型的学习步长为0.000 5，适应优化算法为RMSprop. 验证集上的最佳模型超参数被确定后，使用测试数据来评价模型的泛化程度. 图6所示为随机选取192组未被神经网络学习过的数据，输入到

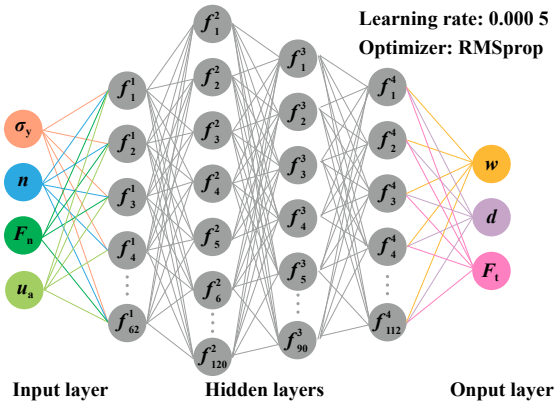

Fig. 5　Optimal MLP structure determined from hyperparametric search, where f_l^q is the l neuron of the qth layer

图 5　从超参数搜索中确定的最优MLP结构，其中f_l^q为第q层的l神经元

已经训练好的MLP神经网络中，将预测的w、d和F_t与实际的值进行比较，并且用决定系数R^2来衡量MLP回归的好坏，如公式(4)所示：

$$R^2=\frac{\sum\left(\hat{y}-\bar{y}\right)^2}{\sum\left(y-\bar{y}\right)^2} \tag{4}$$

MLP对F_t、w和d预测的拟合程度分别为0.947，0.986和0.97. MLP训练过程中分别在训练、验证和测试数据集上的误差列于表3中. 可以看到无论是在训练、验证和测试数据集，MLP对F_t的预测MAPE误差低于11%而对w和d均低于5.3%，说明MLP具有良好的预测性和一定的泛化性.

由图7(a~c)可以看出，在24 N相同法向载荷下，304不锈钢产生的表观深度和划痕宽度最小，说明在24 N法向载荷下304不锈钢材料具有最强的抗划擦性能，18CrNiMo7-6合金钢次之，黄铜最差. 这是因为黄铜抵抗划痕变形的能力与另外2种材料比最弱，而对于304不锈钢屈服应力虽然小于18CrNiMo7-6合金钢，但随着变形的增加，304不锈钢抵抗变形的能力逐渐超过18CrNiMo7-6合金钢，如图4所示. 从图7中可以发现试验结果与MLP预测、有限元仿真和试验结果较为接近. 训练后的MLP神经网络预测的划痕响应与划痕试验对比w、d和F_t相对误差均在11%以内. 表明本文中训练的MLP神经网络可对不同金属材料进行合理的预测. 目前的机器学习模型大多被认为是“黑盒”. 为了解决机器学习模型的“黑盒”问题，相关学者提出了可解释机器学习. 可解释机器学习不仅能给出模型的预测值，还能给出得到该预测值的理由，进而实现

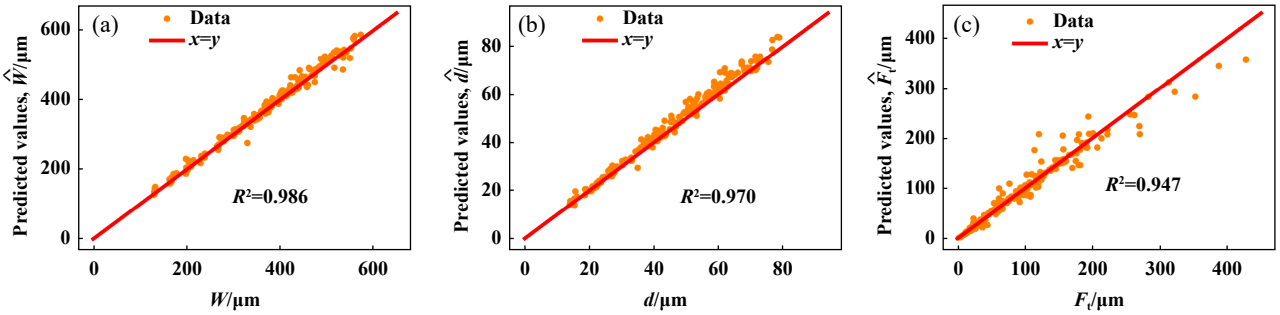

Fig. 6 The plots of MLP testing regression analysis: (a) w; (b) d ; (c) F_t

图 6 MLP测试集回归分析：(a) w；(b) d；(c) F_t

表 3 MLP在训练、验证和测试数据集上的误差

Table 3 Performance of MLP on train, validation and test datasets

Parameters	Train MAPE	Validation MAPE	Test MAPE
w	2.3%	3.1%	3.2%
d	5.2%	3.1%	5.3%
F_t	6.3%	10.8%	10.9%

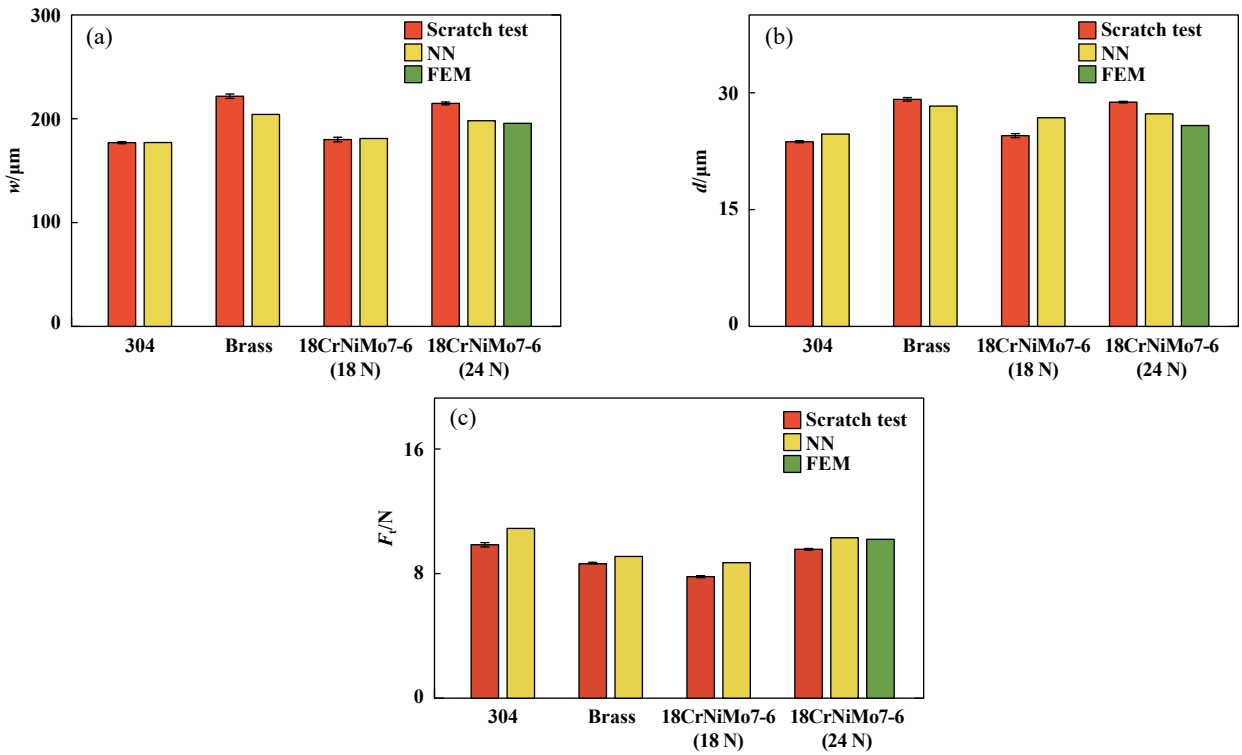

Fig. 7 Comparison between the scratch responses obtained from scratch test and MLP: (a) w; (b) d ; (c) F_t

图 7 划痕试验、MLP预测和有限元仿真划痕响应的对比：(a) w；(b) d；(c) F_t

模型的安全、透明和公平等特性[36]. 这方面的研究具有重要的研究意义和价值，其在划痕领域的应用需要进一步开展研究.

4 结论

a. 本文采用有限元与MLP神经网络的方法，建立不同金属材料力学性能下划痕工况(F_n、μ_a)与划痕响应(w、d和F_t)之间的关系.

b. 对比了3种金属材料(304不锈钢、黄铜和18CrNiMo7-6合金钢)划痕响应与MLP神经网络预测值，w、d和F_t相对误差均在11%以内，验证了本文中训练的MLP神经网络可用于预测不同力学性能材料的划

痕响应并评价其抗划擦性能.

c. 相比于18CrNiMo7-6合金钢和黄铜，在本文研究范围内304不锈钢具有最好的抗划擦性能.

参 考 文 献

[1] Tabor D. The physical meaning of indentation and scratch hardness[J]. British Journal of Applied Physics, 1956, 7(5): 159–166. doi: 10.1088/0508-3443/7/5/301.

[2] Cakmak E, Tekin K C, Malayoglu U, et al. The effect of substrate composition on the electrochemical and mechanical properties of PEO coatings on Mg alloys[J]. Surface and Coatings Technology, 2010, 204(8): 1305–1313. doi: 10.1016/j.surfcoat.2009.10.012.

[3] Zhang C H, Lu X C, Wang H, et al. Microstructure, mechanical properties, and oxidation resistance of nanocomposite Ti-Si-N coatings[J]. Applied Surface Science, 2006, 252(18): 6141–6153. doi: 10.1016/j.apsusc.2005.04.056.

[4] Culha O, Celik E, Ak Azem N F, et al. Microstructural, thermal and mechanical properties of HVOF sprayed Ni-Al-based bond coatings on stainless steel substrate[J]. Journal of Materials Processing Technology, 2008, 204(1-3): 221–230. doi: 10.1016/j.jmatprotec.2007.11.036.

[5] Akono A T, Randall N X, Ulm F J. Experimental determination of the fracture toughness via microscratch tests: application to polymers, ceramics, and metals[J]. Journal of Materials Research, 2012, 27(2): 485–493. doi: 10.1557/jmr.2011.402.

[6] Zhang Dong, Sun Yuan, Gao Chenghui, et al. Measurement of fracture toughness of copper via constant-load microscratch with a spherical indenter[J]. Wear, 2020, 444–445: 203158. doi: 10.1016/j.wear.2019.203158.

[7] Liu Haitao, Zhang Jianwei, Zhao Minghao, et al. Determination of the fracture toughness of glasses via scratch tests with a vickers indenter[J]. Acta Mechanica Solida Sinica, 2022, 35(1): 129–138. doi: 10.1007/s10338-021-00264-6.

[8] Liu Ming, Li Shuo, Gao Chenghui. Fracture toughness measurement by micro-scratch tests with conical indenter[J]. Tribology, 2019, 39(5): 556–564 (in Chinese) [刘明, 李烁, 高诚辉. 利用圆锥压头微米划痕测试材料断裂韧性[J]. 摩擦学学报, 2019, 39(5): 556–564]. doi: 10.16078/j.tribology.2019021.

[9] Bellemare S C, Dao M, Suresh S. A new method for evaluating the plastic properties of materials through instrumented frictional sliding tests[J]. Acta Materialia, 2010, 58(19): 6385–6392. doi: 10.1016/j.actamat.2010.07.060.

[10] Liu Haitao, Zhao Minghao, Lu Chunsheng, et al. Characterization on the yield stress and interfacial coefficient of friction of glasses from scratch tests[J]. Ceramics International, 2020, 46(5): 6060–6066. doi: 10.1016/j.ceramint.2019.11.065.

[11] Liu Ming, Liu Xingjun, Gao Chenghui. Microscratch properties of polycarbonate by spherical indenter[J]. Tribology, 2021, 41(6): 890–901 (in Chinese) [刘明, 刘星君, 高诚辉. 利用球形压头研究聚碳酸酯的微米划痕性能[J]. 摩擦学学报, 2021, 41(6): 890–901]. doi: 10.16078/j.tribology.2020226.

[12] Zhang Yafeng, He Hongtu, Yu Jiaxin, et al. AFM nanoscratch behaviors of three optical glasses used in ICF[J]. Tribology, 2018, 38(3): 349–355 (in Chinese) [张亚锋, 何洪途, 余家欣, 等. 用于ICF的三种典型光学玻璃的AFM纳米划痕行为研究[J]. 摩擦学学报, 2018, 38(3): 349–355]. doi: 10.16078/j.tribology.2018.03.013.

[13] Xu Xiaojun, van der Zwaag S, Xu Wei. The effect of martensite volume fraction on the scratch and abrasion resistance of a ferrite-martensite dual phase steel[J]. Wear, 2016, 348–349: 80–88. doi: 10.1016/j.wear.2015.11.017.

[14] Jiang Han, Browning R, Sue H J. Understanding of scratch-induced damage mechanisms in polymers[J]. Polymer, 2009, 50(16): 4056–4065. doi: 10.1016/j.polymer.2009.06.061.

[15] Gao W M, Wang L, Coffey J K, et al. Finite element simulation of scratch on polypropylene panels[J]. Materials & Design, 2018, 140: 400–408. doi: 10.1016/j.matdes.2017.12.018.

[16] Hossain M M, Jiang H, Sue H J. Effect of constitutive behavior on scratch visibility resistance of polymers—a finite element method parametric study[J]. Wear, 2011, 270(11-12): 751–759. doi: 10.1016/j.wear.2011.01.022.

[17] Jiang H, Lim G T, Reddy J N, et al. Finite element method parametric study on scratch behavior of polymers[J]. Journal of Polymer Science Part B:Polymer Physics, 2007, 45(12): 1435–1447. doi: 10.1002/polb.21169.

[18] Zhang Jianwei, Jiang Han, Jiang Chengkai, et al. Experimental and numerical investigations of evaluation criteria and material parameters' coupling effect on polypropylene scratch[J]. Polymer Engineering & Science, 2018, 58(1): 118–122. doi: 10.1002/pen.24538.

[19] Pöhl F, Hardes C, Theisen W. Scratch behavior of soft metallic materials[J]. AIMS Materials Science, 2016, 3(2): 390–403. doi: 10.3934/matersci.2016.2.390.

[20] Liu Ming, Wang Wei. Effects of sliding velocity on microscratch responses of thermoplastics by Berkovich indenter[J]. Polymer Bulletin, 2023, 80(7): 7901–7926. doi: 10.1007/s00289-022-04397-7.

[21] Hornik K, Stinchcombe M, White H. Multilayer feedforward networks are universal approximators[J]. Neural Networks, 1989, 2(5): 359–366. doi: 10.1016/0893-6080(89)90020-8.

[22] LeCun Y, Bengio Y, Hinton G. Deep learning[J]. Nature, 2015, 521(7553): 436–444. doi: 10.1038/nature14539.

[23] Spencer B F, Hoskere V, Narazaki Y. Advances in computer vision-based civil infrastructure inspection and monitoring[J]. Engineering, 2019, 5(2): 199–222. doi: 10.1016/j.eng.2018.11.030.

[24] Young T, Hazarika D, Poria S, et al. Recent trends in deep learning based natural language processing[review article[J]. IEEE Computational Intelligence Magazine, 2018, 13(3): 55–75. doi: 10.1109/MCI.2018.2840738.

[25] Liu Xing, Athanasiou C E, Padture N P, et al. A machine learning

approach to fracture mechanics problems[J]. Acta Materialia, 2020, 190: 105–112. doi: 10.1016/j.actamat.2020.03.016.

[26] Lu Lu, Dao Ming, Kumar P, et al. Extraction of mechanical properties of materials through deep learning from instrumented indentation[J]. Proceedings of the National Academy of Sciences of the United States of America, 2020, 117(13): 7052–7062. doi: 10.1073/pnas.1922210117.

[27] Xie Haibo, Wang Zhanjiang, Qin Na, et al. Prediction of friction coefficients during scratch based on an integrated finite element and artificial neural network method[J]. Journal of Tribology, 2020, 142(2): 021703. doi: 10.1115/1.4045013.

[28] Chu J, Rumao L, Coleman B. Scratch and mar resistance of filled polypropylene materials[J]. Polymer Engineering & Science, 1998, 38(11): 1906–1914. doi: 10.1002/pen.10361.

[29] Liu Ming, Li Guoxiang, Zhou Chao, et al. Analysis of 3D morphology and scratch hardness of copper under large constant load[J]. Tribology, 2021, 41(4): 467–73 (in Chinese) [刘明, 李国翔, 周超, 等. 恒定大载荷划痕试验下紫铜的三维形貌及划痕硬度分析[J]. 摩擦学学报, 2021, 41(4): 467–73]. doi: 10.16078/j.tribology.2020140.

[30] Zhang Jianwei, Li Yuanxin, Zheng Xuefeng, et al. Determination of plastic properties of surface modification layer of metallic materials from scratch tests[J]. Engineering Failure Analysis, 2022, 142: 106754. doi: 10.1016/j.engfailanal.2022.106754.

[31] Liu Ming, Wu Jianan. Scratch behavior of materials under progressive load by conical indenter[J]. Chinese Journal of Materials Research, 2022, 36(3): 191–205 (in Chinese) [刘明, 伍家楠. 圆锥压头递增载荷对材料的划痕行为[J]. 材料研究学报, 2022, 36(3): 191–205]. doi: 10.11901/1005.3093.2021.219.

[32] Bellemare S, Dao M, Suresh S. The frictional sliding response of elasto-plastic materials in contact with a conical indenter[J]. International Journal of Solids and Structures, 2007, 44(6): 1970–1989. doi: 10.1016/j.ijsolstr.2006.08.008.

[33] Hollomon J H. Tensile deformation[J]. Metals Technology, 1945, 12: 268–290.

[34] Akiba T, Sano S, Yanase T, et al. Optuna: a next-generation hyperparameter optimization framework[C]//Proceedings of the 25th ACM SIGKDD International Conference on Knowledge Discovery & Data Mining. Anchorage, AK, USA. New York: ACM, 2019: 2623–2631. doi: 10.1145/3292500.3330701.

[35] Paszke A, Gross S, Massa F, et al. PyTorch: an imperative style, high-performance deep learning library"[EB/OL]. 2019: arXiv: 1912.01703. https://doi.org/10.48550/arXiv.1912.01703.

[36] Zhang Yu, Tiňo P, Leonardis A, et al. A survey on neural network interpretability[J]. IEEE Transactions on Emerging Topics in Computational Intelligence, 2021, 5(5): 726–742. doi: 10.1109/TETCI.2021.3100641.